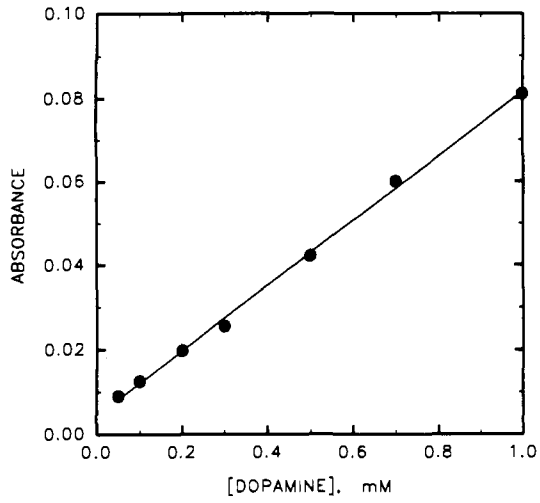

Figure 9. Charge-transfer absorbance (at 464 nm) of Nafion membranes (0.180 mm) preloaded with 1^{4+} after 15 min of exposure to phosphate buffer solutions (pH = 7) containing variable concentrations of dopamine.

in solutions of varying dopamine concentrations. The measured absorbance is linearly related to the dopamine concentration. Linear absorbance vs concentration plots were also obtained with indole, catechol, serotonin, and norepinephrine. The slopes of these straight lines were all similar; 1.0 mM solutions of any of the surveyed guests produce membrane absorbances in the range 0.08–0.14. However, in the cases of serotonin and norepinephrine, longer immersion (loading) times were needed to reach this absorbance range. Specifically, loading periods of 25 min and 3 h were needed in our experiments with serotonin and norepinephrine, respectively. In contrast, dopamine, indole, and catechol gave rise to absorbance values in the indicated range with shorter loading times of 15 min in all three cases. Although the origin of these loading time differences is still unclear, these experiments clearly offer additional evidence for the formation of charge-transfer complexes inside Nafion between the surveyed guests and 1^{4+}. Furthermore, the linearity of the absorbance values as a function of the guest concentration in the loading solution can be utilized for analytical purposes as a method to determine these neurotransmitters, as well as catechol, indole, and probably other neutral or cationic compounds possessing electron-rich aromatic rings. We are currently exploring in detail the potential of this simple analytical methodology for the determination of compounds with biological significance.

Conclusions

This work has shown that receptor 1^{4+} has a substantial affinity for the surveyed neurotransmitters, indole, and catechol, forming inclusion complexes with all of them in aqueous media. The origin of these binding properties dwells in the rigid π-acceptor cavity (defined by the two paraquat groups) of the title cyclophane. We have also shown that it is possible to manipulate the oxidation state of the receptor's paraquat groups to alter its affinity for π-donor guests. Thus, this species provides the first reported example of a redox-switchable molecular receptor. The tetracationic nature of the receptor makes possible its stable incorporation in a polyelectrolyte Nafion matrix where it also binds the same guests as concluded from our electrochemical and spectrophotometric studies. However, improved methods for the immobilization of this receptor—or structurally related ones—on electrode surfaces are required for the design and construction of practical sensor devices for biochemically relevant species.

Acknowledgment. The support of this research by the NSF (Grant CHE-9000531) is gratefully acknowledged. We thank Timothy T. Goodnow for performing some preliminary experiments and the Eastman Kodak Co. for the donation of the BAS-100 electroanalyzer.

Long-Range Spin Density Propagation in Saturated Hydrocarbons: 3-[*n*]Staffyl Radicals

Allan J. McKinley, Prabha N. Ibrahim, V. Balaji, and Josef Michl*,[1]

Contribution from the Department of Chemistry and Biochemistry, University of Colorado, Boulder, Colorado 80309-0215. *Received May 8, 1992*

Abstract: The bridgehead radicals derived from the first three [*n*]staffanes (n = 1–3), oligomers of [1.1.1]propellane, have been generated from the corresponding bromides, and their solution EPR spectra have been recorded. Remarkably long-range hyperfine coupling has been found to ϵ, ζ, and even ι hydrogens, in qualitative agreement with ab initio UHF calculations. The coupling to the bridgehead hydrogen is attenuated by a factor of about 25 per added bicyclo[1.1.1]pentane cage. The long-range propagation of spin density can be attributed to strong interaction between the orbitals used to make the exocyclic bonds in the 1 and 3 positions of each bicyclo[1.1.1]pentane cage. The situation can be understood simply in terms of a linear σ-hyperconjugated chain of orbitals interacting through resonance integrals whose effective magnitude alternates in an about 1:5 ratio. A more detailed analysis is provided by considering the effect on the spin density of the various types of off-diagonal elements in the UHF Hartree–Fock matrix expressed in terms of maximally spin-paired natural bond orbitals (MSP-NBO). This permits a clean separation of through-space and through-bond interactions as well as further separation of each of these into contributions due to bond delocalization and those due to bond spin polarization.

Introduction

Inert and relatively rigid linear molecules terminated with axial substituents and available in a selection of lengths with small increments, such as the functionalized oligomers **1** of [1.1.1]-propellane (**2**), called [*n*]staffanes for short, have been proposed as building elements of a molecular engineering construction set of the "Tinkertoy" type.[2,3] [*n*]Staffanes[4] and their terminally

(1) This project was initiated at the University of Texas, Austin, Texas.

(2) Kaszynski, P.; Michl, J. *J. Am. Chem. Soc.* **1988**, *110*, 5225. Michl, J.; Kaszynski, P.; Friedli, A. C.; Murthy, G. S.; Yang, H.-C.; Robinson, R. E.; McMurdie, N. D.; Kim, T. In *Strain and Its Implications in Organic Chemistry*; de Meijere, A., Blechert, S., Eds.; NATO ASI Series, Kluwer Academic Publishers: Dordrecht, The Netherlands, 1989; p 463, Vol. 273.

0002-7863/92/1514-10631$03.00/0

functionalized derivatives[5] have been characterized structurally and more recently, also with respect to mechanical (vibrational) properties,[6] but little is known about the propagation of electronic influences such as spin density delocalization through them.[7]

Photoelectron spectra of the first five members of the hydrocarbon series[3,8] and of numerous substituted derivatives[8,9] have been measured. These spectra and a fair number of prior results of measurement of NMR coupling constants in monomeric[10] and dimeric[2,3] bicyclo[1.1.1]pentanes as well as studies of their chemical reactivity[11,12] suggest very strongly that there is considerable transannular and/or through-bond interaction between the orbitals used to make the exocyclic bonds in positions 1 and 3 of the bicyclo[1.1.1]pentane cage. Through-space transannular interaction clearly cannot help but be strong, since, after all, the separation of the carbon atoms in positions 1 and 3 is only about 1.85 Å,[4,5] and the back lobes of the two orbitals are aimed directly at each other.

These orbitals have considerable *s* character, as expected from the bond angles and Bent's rules[13] and as reflected in the one-bond $J_{^{13}CH}$ NMR coupling constant,[10a,14] in the short lengths[4,5] and high vibrational frequencies[6] of the exocyclic bonds, in the acidity of the bridgehead hydrogens,[12,15] and in various other aspects of their chemical reactivity. Not surprisingly, the transannular interaction is strongest when exocyclic substituents in the bridgehead positions are absent altogether, i.e., in [1.1.1]propellane (**2**), in which the two orbitals are used to describe a regular two-electron bond. In **2**, the intercarbon distance is only 1.596 Å,[16] and probably the simplest, albeit rather approximate, way to view the strange direction of the transannular bond at the inverted carbons is to say that it is formed primarily by the nondirectional 2*s* orbitals, while the remaining three bonds on each, oriented very roughly at right angles to each other, are formed primarily by the three 2*p* orbitals.

Perhaps the most eloquent evidence for strong interaction between the two bridgehead positions in bicyclo[1.1.1]pentane is provided by the enormous magnitude of the hyperfine coupling constant of the γ (bridgehead) hydrogen in the bicyclo[1.1.1]-pent-1-yl bridgehead radical (**3**, $n = 1$). The reported[17] value is 69.6 G, about one-seventh of the hyperfine coupling constant in a free hydrogen atom. This is about three times the value for bicyclo[2.1.1]hex-1-yl and one to two orders of magnitude more than the γ coupling constants in other saturated radicals.[18] In simple molecular orbital terms, the two σ-symmetry orbitals on the carbons and the 1*s* orbital on the bridgehead hydrogen form a linear system analogous to that of an allyl radical, with a strong C–H and a weaker C–C resonance integral. In simple valence-bond terms, usually invoked for the interpretation of EPR coupling constants attributed to hyperconjugation, the long-bond resonance structure **4** has considerable weight.

By either of these arguments, one would expect the transannular C–C separation to be somewhat smaller, and the C–H bond length somewhat longer, in the radical **3** ($n = 1$) than in bicyclo-[1.1.1]pentane (**1**, X = Y = H, $n = 1$) itself. In the extreme, the radical can be viewed in the sense of the resonance structure **4** as a complex of a hydrogen atom with [1.1.1]propellane, just as the corresponding bridgehead cation, bicyclo[1.1.1]pent-1-yl, can be viewed at its unstable symmetrical geometry with a 3-fold axis as a complex of a proton with [1.1.1]propellane, in order to understand simply the extraordinary ease of its formation from bicyclo[1.1.1]pentanes containing a leaving group in the bridgehead position.[19] Adoption of this simple viewpoint for the bicyclo[1.1.1]pent-1-yl radical also makes it easy to rationalize the reversibility of radical addition to [1.1.1]propellane,[11] the selectivities of radical abstraction reactions on bicyclo[1.1.1]pentane and its derivatives,[17,20] and other aspects of their radical chemistry.

Although the EPR results for the bicyclo[1.1.1]pent-1-yl radical **3** ($n = 1$) suggest that the propagation of spin density through longer [*n*]staffane rods with a bridgehead radical center will be facile as well, they do not provide a quantitative guide for the attenuation of this effect with the number of cages *n*. The attenuation factor of 7 for spin density upon going from an H atom to its "adduct with [1.1.1]propellane", **3** ($n = 1$), need not be the same as those for going to its formal adduct with two or more [1.1.1]propellanes, as one proceeds to the higher members of the [*n*]staffyl radical series, **3** ($n = 2, 3...$). First, the propensity of the C–H and C–C bonds toward hyperconjugation need not be the same. Second, the interbridgehead C–C distance is likely to be close to 1.85 Å in the cages that are more distant from the radical center, while semiempirical calculations[21] suggest that in the cage that carries the radical center, it is shorter and thus more conducive to strong hyperconjugation.

We have now generated and studied the first three members of the [*n*]staff-3-yl series **3** in order to obtain an understanding of the way in which the bridgehead spin density propagates through the [*n*]staffane skeleton. This ought to provide a helpful indication of the general ease of propagation of electronic influences of σ-symmetry through this intended basic building block of the planned molecular construction set. Specifically, it will provide an estimate for the attenuation of the expected antiferromagnetic coupling between atoms attached to the two bridgehead positions.

We have analyzed the results both in the simple terms outlined in this introductory section and at a more detailed albeit still very approximate UHF level in terms of natural bond orbitals. This permits a separation of through-space and through-bond contributions as well as bond spin polarization and bond delocalization parts of each.

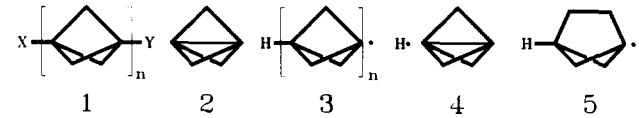

1 2 3 4 5

Experimental Section

Materials. Melting points were determined using a Mel-Temp apparatus and are uncorrected. NMR spectra were run at 360 MHz on a

(3) Kaszynski, P.; Friedli, A. C.; Michl, J. *J. Am. Chem. Soc.* **1992**, *114*, 601.

(4) Murthy, G. S.; Hassenrück, K.; Lynch, V. M.; Michl, J. *J. Am. Chem. Soc.* **1989**, *111*, 7262.

(5) Friedli, A. C.; Lynch, V. M.; Kaszynski, P.; Michl, J. *Acta Crystallogr.* **1990**, *B46*, 377.

(6) Gudipati, M. S.; Hamrock, S. J.; Balaji, V.; Michl, J. *J. Phys. Chem.*, in press.

(7) Kramer, L. S.; Clauss, A. W.; Francesconi, L. C.; Corbin, D. R.; Hendrickson, D. N.; Stucky, G. D. *Inorg. Chem.* **1981**, *20*, 2070.

(8) Gleiter, R.; Pfeifer, K.-H.; Szeimies, G.; Bunz, U. *Angew. Chem., Int. Ed. Engl.* **1990**, *29*, 413.

(9) David, D. E.; Murthy, G. S.; Hassenrück, K.; Friedli, A. C.; Kaszynski, P.; Michl, J., unpublished results.

(10) (a) Wiberg, K. B.; Connor, D. S. *J. Am. Chem. Soc.* **1966**, *88*, 4437. (b) Della, E. W.; Gangodawila, H.; Pigou, P. E. *J. Org. Chem.* **1988**, *53*, 592. Barfield, M.; Della, E. W.; Pigou, P. E.; Walter, S. R. *J. Am. Chem. Soc.* **1982**, *104*, 3550. Della, E. W.; Kasum, B.; Kirkbride, K. P. *J. Am. Chem. Soc.* **1987**, *109*, 2746, and references therein.

(11) McGarry, P. F.; Johnston, L. J.; Scaiano, J. C. *J. Org. Chem.* **1989**, *54*, 6133.

(12) Della, E. W.; Taylor, D. K.; Tsanaktsidis, J. *Tetrahedron Lett.* **1990**, *31*, 5219.

(13) Bent, H. A. *Chem. Rev.* **1961**, *61*, 275.

(14) Della, E. W.; Cotsaris, E.; Hine, P. T.; Pigou, P. E. *Aust. J. Chem.* **1981**, *34*, 913.

(15) Graul, S. T.; Squires, R. R. *J. Am. Chem. Soc.* **1990**, *112*, 2517.

(16) Hedberg, L.; Hedberg, K. *J. Am. Chem. Soc.* **1985**, *107*, 7257.

(17) Maillard, B.; Walton, J. C. *J. Chem. Soc., Chem. Commun.* **1983**, 900.

(18) King, F. W. *Chem. Rev.* **1976**, *76*, 157. Walton, J. C. *Chem. Soc. Rev.* **1992**, *21*, 105.

(19) (a) Della, E. W.; Gill, P. M. W.; Schiesser, C. H. *J. Org. Chem.* **1988**, *53*, 4354. (b) Wiberg, K. B.; Hadad, C. M.; Sieber, S.; Schleyer, P. v. R. *J. Am. Chem. Soc.* **1992**, *114*, 5820.

(20) Robinson, R. E.; Michl, J. *J. Org. Chem.* **1989**, *54*, 2051, and references therein.

(21) Ohsaku, M.; Imamura, A.; Hirao, K.; Kawamura, T. *Tetrahedron* **1979**, *35*, 701. Bews, J. R.; Glidewell, C.; Walton, J. C. *J. Chem. Soc., Perkin Trans. 2* **1982**, 1447.

Nicolet NT-360 instrument or at 250 MHz on a Bruker AC-250 instrument in $CDCl_3$. Infrared spectra were recorded on a Nicolet 60SXR FTIR instrument in $CDCl_3$, unless specified otherwise.

[n]Staffane-3-carboxylic acids (**1**, n = 1–3, X = H, Y = COOH) were synthesized by the oxidation of 3(1-ethoxyethyl)[n]staffanes obtained by the photolysis of a solution of **2** in ether in the presence of benzoyl peroxide.[3] 2-Mercaptopyridine-1-oxide was purchased in the form of its sodium salt (Barton reagent) from Fluka and vacuum dried before use. 1-Bromo-1-chloro-2,2,2-trifluoroethane, thionyl chloride, di-*tert*-butyl peroxide, triethylsilane, and cyclopentane were purchased from Aldrich, cyclopropane from Matheson. *tert*-Butyl 3-(methoxycarbonyl)bicyclo-[1.1.1]pentane-1-peroxycarboxylate[22] (**1**, n = 1, X = COOMe, Y = COO*t*Bu) was prepared according to the literature procedure, as was 1-bromobicyclo[1.1.1]pentane[23] (**1**, n = 1, X = H, Y = Br). The bromide was fairly sensitive to moisture and decomposed on alumina and silica gel (^{1}H NMR δ 2.26 (s, 6 H) 3.15 (s, 1 H); ^{13}C NMR δ 28.57, 38.49, 58.28). It also partially decomposed thermally during preparative GC. The main decomposition product appeared to be 3-methylenecyclobutyl bromide (^{1}H NMR δ 3.14 (m, 2 H), 3.33 (m, 2 H), 4.42 (q, 1 H), 4.83 (q, 2 H); ^{13}C NMR δ 36.94, 45.38, 107.26, 142.37).

3-Bromo[2]staffane (1, n = 2, X = H, Y = Br). [2]Staffane-3-carboxylic acid (300 mg, 1.685 mmol) was refluxed with freshly distilled thionyl chloride (5 mL) for 6 h. Excess thionyl chloride was evaporated in a rotatory evaporator, and the crude acid chloride was purified by Kugelrohr distillation (120 °C, 0.6 mmHg, 300 mg, 91% yield) [^{1}H NMR δ 1.67 (s, 6 H), 1.99 (s, 6 H), 2.42 (s, 1 H); ^{13}C NMR δ 26.77, 39.38, 43.79, 44.63, 49.24, 51.79, 171.22; IR 1700, 1210 cm^{-1}]. Vacuum-dried (100 °C, 45 min) sodium salt of 2-mercaptopyridine-1-oxide (Barton reagent) (300 mg, 2 mmol) cooled under argon was mixed with 1-bromo-1-chloro-2,2,2-trifluoroethane (2 mL) and stirred. The acid chloride (300 mg, 1.53 mmol) was dissolved in 4 mL of the solvent and added to the suspension of the Barton reagent. The mixture was refluxed with concurrent irradiation with a sunlamp for 3 h. The suspension was filtered, and the filtrate was evaporated. The residue (676 mg) was found by NMR to be a ~1:1 mixture of 1-chloro-2,2,2-trifluoroethyl 2-pyridyl sulfide and 3-bromo[2]staffane. The latter was isolated by recrystallization from pentane (137 mg, 42% yield): mp 84 °C; ^{1}H NMR δ 1.66 (s, 6 H), 2.07 (s, 6 H), 2.41 (s, 1 H); ^{13}C NMR δ 26.88, 37.52, 41.44, 43.74, 49.78, 57.72; IR 2971, 2901, 2865, 1217 cm^{-1}; CIMS (*i*-C_4H_{10}), m/z 133 (M – Br, 30), 105 (100), 93 (25), 91 (100), 81 (5), 79 (60), 67 (20). Anal. Calcd for $C_{10}H_{13}Br$: C, 56.34; H, 6.10, Br, 37.56. Found: C, 56.29; H, 6.13; Br, 37.49.

3-Bromo[3]staffane (1, n = 3, X = H, Y = Br). The same procedure was followed. [3]Staffane-3-carboxylic acid (120 mg, 0.492 mmol) was converted to the corresponding acid chloride (125 mg, 97% yield) [^{1}H NMR δ 1.45 (s, 6 H), 1.60 (s, 6 H), 1.98 (s, 6 H), 2.38 (s, 1 H); ^{13}C NMR δ 26.45, 36.91, 38.64, 39.30, 44.66, 44.88, 47.93, 49.08, 51.66, 171.38; IR 1703, 1210 cm^{-1}]. The chloride (110 mg, 0.42 mmol) was treated with Barton reagent (150 mg, 1 mmol) in 1-bromo-1-chloro-2,2,2-trifluoroethane to obtain 220 mg of an about 1:1 mixture of 1-chloro-2,2,2-trifluoroethyl 2-pyridyl sulfide and 3-bromo[3]staffane. Recrystallization from pentane yielded the latter in pure form (70 mg, 60%): mp 108 °C; ^{1}H NMR δ 1.44 (s, 6 H), 1.59 (s, 6 H), 2.05 (s, 6 H), 2.38 (s, 1 H); ^{13}C NMR δ 26.46, 37.02, 37.62, 38.78, 41.26, 44.82, 48.49, 49.10, 57.62; IR 2964, 2901, 2866, 1210 cm^{-1}; CIMS (*i*-C_4H_{10}), m/z 199 (M – Br, 10), 157 (50), 143 (90), 129 (70), 105 (80), 93 (75), 91 (100), 81 (40), 79 (80), 67 (45). Anal. Calcd for $C_{15}H_{19}Br$: C, 64.52; H, 6.81; Br, 28.67. Found: C, 64.53; H, 6.85; Br, 28.57.

Spectroscopic Procedures. The bridgehead [n]staff-3-yl radicals **3** were generated from the bromides in the usual manner[24] by continuous low-temperature UV irradiation of a quartz cell containing a solution of a [n]staff-3-yl bromide in a 1:1:4 mixture of di-*tert*-butyl peroxide, triethylsilane, and either cyclopropane or cyclopentane, located in the EPR cavity. The irradiation source was a tightly focused 1 kW high-pressure mercury-xenon lamp (Oriel) filtered by a water filter and a Corning 7-54 UV transmitting filter. The di-*tert*-butyl peroxide was purified using a literature method,[25] and the other reagents were distilled before use. The solutions were thoroughly degassed by several freeze–pump–thaw cycles.

EPR spectra were recorded on a Bruker ESP-300 spectrometer. Absolute g values were determined by the use of a Bruker ER035M NMR gaussmeter and in-cavity probe to measure the magnetic field at the sample and a Hewlett-Packard 5350A frequency counter to measure the spectrometer frequency. Spectral simulations were performed on an IBM-compatible personal computer.

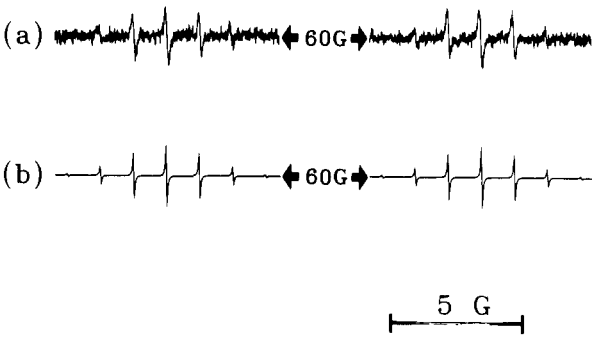

Figure 1. (a) Measured and (b) computer simulated EPR spectrum of [1]staff-3-yl (**3**, n = 1) in cyclopentane at 200 K.

In the case of the [1]staff-1-yl radicals the spectrometer had a magnet with poor field homogeneity resulting in an instrumentally limited line width of about 120 mG. Since its EPR spectrum had been already reported,[17] this was considered acceptable.

Calculations. The geometries of bridgehead [n]staffyl radicals (**3**, n = 1–3) were optimized under a C_{3v} symmetry constraint at the unrestricted Hartree–Fock (UHF) level using the 6-31G* basis set. Second derivatives of the energy were calculated for the n = 1 and 2 radicals, to ensure that the optimized geometries correspond to a local minimum in the potential energy surface. The Fermi contact terms for the hydrogen atoms were obtained for the optimized geometries and converted to the hyperfine coupling constant by multiplication with the factor 1596.9, obtained from fundamental physical constants.[26] The spin contamination of the doublet UHF wave function was found to be negligible. These calculations were carried out using the Gaussian 88[27] program running on an IBM RS-6000/550 computer at the University of Colorado at Boulder. The program for natural bond orbital analysis was obtained from Prof. F. Weinhold (University of Wisconsin, Madison). It was modified to permit the computation of maximally spin-paired ROHF natural bond orbitals by averaging of the ordinary spin-polarized electron densities, to permit the UHF Fock matrix to be written in this basis for the investigation of the effect of the deletion and retention of selected off-diagonal elements, and to compute the Fermi contact terms from the spin densities obtained from the modified UHF Fock matrix.

Results

[n]Staff-3-yl radicals (**3**, n = 1–3) were generated by abstraction of a bromine atom from a 3-bromo[n]staffane by the triethylsilyl radical, and their EPR spectra were recorded (Figures 1a–3a). For n = 1, the solvent used was cyclopentane at 200 K. For n = 2 and 3, the [n]staff-3-yl radicals were not observed under these conditions. However, if cyclopropane was used as the solvent at 140 K, they were observed. In all cases blocking the irradiation resulted in an immediate loss of the EPR signal.

UV irradiation of a perester, *tert*-butyl 3-(methoxycarbonyl)[1]staffane-1-peroxycarboxylate (**1**, n = 1, X = MeOCO, Y = CO_2Ot-Bu), in cyclopentane solution at 200 K was also tried as a possibly more direct and convenient route to the bridgehead radicals. Strong signals from cyclopentyl radicals were observed, but there was little if any indication of the formation of the expected bridgehead radical. The cyclopentyl radicals obviously resulted from hydrogen abstraction from the solvent by the *tert*-butoxy radicals. This indicated that the peroxide bond was being cleaved by the irradiation as intended, and the weakness of the bridgehead radical signals implies that the decarboxylation step was too slow at this temperture. The EPR spectra of oxygen-centered radicals tend to be rather broad in solution due to

(22) Kaszynski, P.; McMurdie, N. D.; Michl, J. *J. Org. Chem.* **1991**, *56*, 307.

(23) Della, E. W.; Taylor, D. K. *Aust. J. Chem.* **1990**, *43*, 945.

(24) Hudson, A.; Jackson, R. A. *J. Chem. Soc., Chem. Commun.* **1969**, 1323.

(25) Perrin, D. D.; Armarego, W. L. F.; Perrin, D. R. *Purification of Laboratory Chemicals*; Pergmon Press: New York, 1966.

(26) Weltner, W., Jr. *Magnetic Atoms and Molecules*; Van Nostrand Reinhold Company, Inc.: New York, 1983; p 14. *A Physicist's Desk Reference*; Anderson, H. L., Ed.; American Institute of Physics: New York, 1989; p 4.

(27) Frisch, M. J.; Head-Gordon, M.; Schlegel, H. B.; Raghavachari, K.; Binkley, J. S.; Gonzalez, C.; Defrees, D. J.; Fox, D. J.; Whiteside, R. A.; Seeger, R.; Melius, C. F.; Baker, J.; Martin, R. L.; Kahn, L. R.; Stewart, J. J. P.; Fluder, E. M.; Topiol, S.; Pople, J. A. *Gaussian 88 (AIX version)*; Gaussian, Inc.: Pittsburgh, PA.

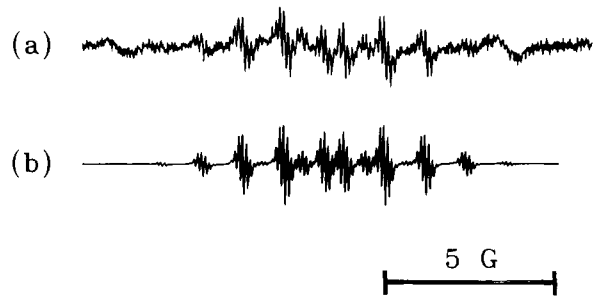

Figure 2. (a) Measured and (b) computer simulated EPR spectrum of [2]staff-3-yl (3, n = 2) in cyclopropane at 140 K.

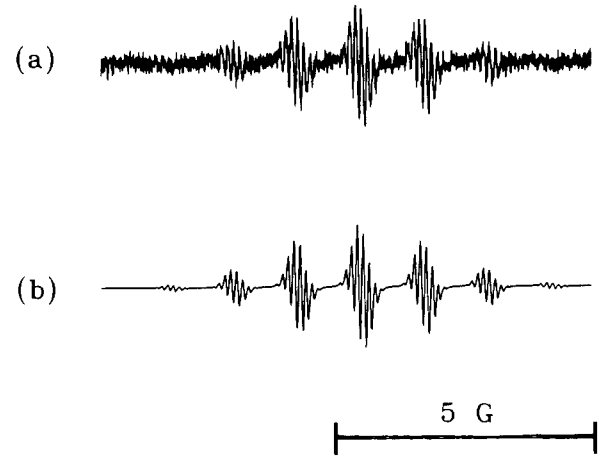

Figure 3. (a) Measured and (b) computer simulated EPR spectrum of [3]staff-3-yl (3, n = 3) in cyclopropane at 140 K.

incomplete motional averaging of the g anisotropy and therefore difficult to observe.

The spectrum of the [1]staff-1-yl radical (3, n = 1, Figure 1a) is in good agreement with that reported previously[17] for the radical generated by hydrogen abstraction from bicyclo[1.1.1]pentane with *tert*-butoxy radicals. It consists of a large doublet (69.4 G, lit.[17] 69.6 G) of septets (1.3 G, lit.[17] 1.2 G). The first and the last line of each group of septets are very weak and can be barely resolved from the noise. The large splitting constant has been assigned[17] to the bridgehead (γ) hydrogen and the small one to the six bridge (β) hydrogens. A computer simulation (Figure 1b) agrees well with the experimental spectrum.

The spectrum of the [2]staff-3-yl radical (3, n = 2, Figure 2a) is a doublet (3.0 G) of septets (1.2 G) of septets (0.1 G). The first and last lines of the septets are once again barely resolved from noise. The splitting constant of 3.0 G is assigned to the bridgehead (ζ) hydrogen, the 1.2 G constant to the six bridge (β) hydrogens in the radical center carrying cage, and the 0.1 G constant to the six bridge (ϵ) hydrogens in the terminal cage. This assignment is based on the assumption that the β hydrogens of the [1]staff-1-yl radicals are essentially equivalent to the β hydrogens of the [2]staff-3-yl radicals. The computer simulation is shown in Figure 2b and agrees very well with the experimental spectrum.

Finally, the spectrum of the [3]staff-3-yl radical (3, n = 3, Figure 3a) is a septet (1.2 G) of octets (0.1 G). As before, the outside lines of the septets are barely resolved from noise. The octet is taken to be a doublet of overlapping septets, with the splitting constants for the doublet and the septet accidentally essentially identical. In analogy with the assignment of the EPR spectra of the [1]staff-1-yl and [2]staff-3-yl radicals, the splitting constant of 1.2 G is assigned to the six bridge (β) hydrogens on the radical center carrying cage. The six bridge (ϵ) hydrogens on the second cage, as well as the bridgehead (ι) hydrogen on the third cage are attributed to a coupling constant of 0.1 G. The coupling with the six bridge (θ) hydrogens on the terminal cage appears to be too small to be resolved in the EPR spectrum. Considering the line width of the EPR spectrum and the expected 6-fold multiplicity, the splitting constant must be less than 0.007 G. The computer simulation (Figure 3b) again is in excellent agreement with the experimental spectrum.

Table I. Measured and Calculated Hyperfine Coupling Constants a_H for [n]Staff-3-yl Radicals 3[a]

	bridge hydrogens			bridghead hydrogen		
n	$a_H\beta$	$a_H\epsilon$	$a_H\theta$	$a_H\gamma$	$a_H\zeta$	$a_H\iota$
			Measured (EPR)			
1	1.3			69.5		
2	1.2	0.1			3.0	
3	1.2	0.1	<0.007			0.1
			Calculated (UHF/6-31G*)			
1	1.2			56.5		
2	1.1	0.02			2.0	
3	1.1	0.01	0.000			0.05

[a] g value: 2.0025 (2).

Table II. Contributions of Fock Matrix Elements (MSP-NBO Basis) to Bridgehead Proton Spin Density

off-diagonal Fock matrix elements retained[a]	a_H[b]	off-diagonal Fock matrix elements retained[a]	a_H[b]	off-diagonal Fock matrix elements retained[a]	a_H[b]
none	0.02	gem TBD[f]	2.36	TBD + TBP	6.91
TSP[c]	32.6	peri TBD[f]	1.95	TBD + TSP	39.0
TBP[d]	0.05	TBP + TSP	32.7	gem TBD[f] + TSP	35.4
TSD[e]	6.88	TSD + TBD	28.6	peri TBD[f] + TSP	34.2
TBD[f]	6.45	TSD + TSP	39.5	all[g]	56.5

[a] All diagonal elements were always kept. NBO notation: R is the occupied (α) and R* is the vacant (β) spin orbital on the radical center; σ_{CH} is the bonding and σ^*_{CH} the antibonding natural orbital of the bridgehead CH bond; σ_{12}, σ_{14}, and σ_{15} are the bonding and σ^*_{12}, σ^*_{14}, and σ^*_{15} are the antibonding natural orbitals of the CC bonds adjacent to the radical center; σ_{23}, σ_{43}, and σ_{53} are the bonding and σ^*_{23}, σ^*_{43}, and σ^*_{53} are the antibonding orbitals of the CC bonds adjacent to the bridgehead CH bond. [b] Hyperfine coupling constant of the bridgehead hydrogen, in G. [c] Through-space spin polarization elements: σ_{CH}–σ^*_{CH}. [d] Through-bond spin polarization elements: σ_{12}–σ^*_{12}, σ_{23}–σ^*_{23}, and those related by symmetry. [e] Through-space delocalization elements: R–σ_{CH}, R–σ^*_{CH}, R*–σ_{CH}, and R*–σ^*_{CH}. [f] Through-bond delocalization elements: R–σ_{12}, R–σ^*_{12}, R*–σ_{12}, R*–σ^*_{12}, σ_{12}–σ_{23}, σ^*_{12}–σ_{23}, σ_{12}–σ^*_{23}, σ^*_{12}–σ^*_{23}, σ_{CH}–σ_{23}, σ_{CH}–σ^*_{23}, σ^*_{CH}–σ_{23}, σ^*_{CH}–σ^*_{23}, and those related by symmetry (geminal), R–σ_{23}, R–σ^*_{23}, R*–σ_{23}, R*–σ^*_{23}, σ_{CH}–σ_{12}, σ_{CH}–σ^*_{12}, σ^*_{CH}–σ_{12}, σ^*_{CH}–σ^*_{12}, and those related by symmetry (perivalent). [g] Identical to the result of ordinary UHF calculation.

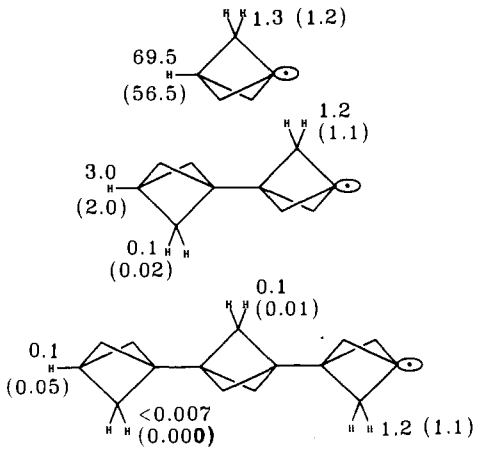

Figure 4. Measured and calculated (UHF/6-31G*, in parentheses) hyperfine coupling constants a_H (G).

The g values of all the above radicals were 2.0025 (2). The measured EPR parameters are summarized in Table I and Figure 4, which also show the results of the UHF calculation of the coupling constants of the hydrogens. Table II compares a series of coupling constant values obtained for the bridgehead hydrogen in 3 (n = 1) upon retention of selected off-diagonal elements in

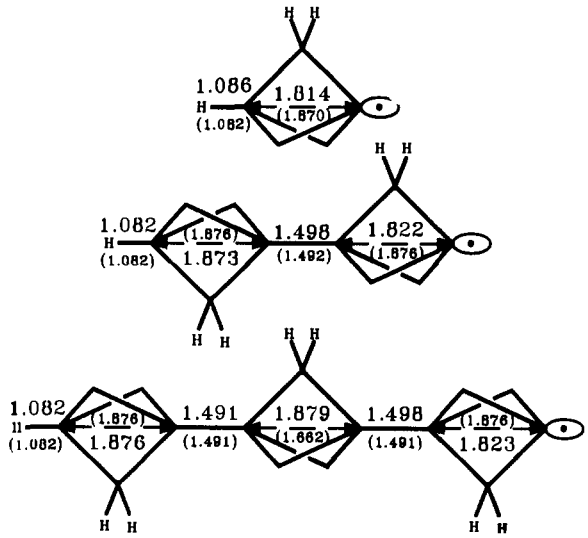

Figure 5. Internuclear distances obtained from the geometries optimized at UHF/6-31G* level. For comparison, the internuclear distances in the parent dihydro compounds, obtained from the geometries optimized at RHF/6-31G* level, are given in parentheses.

the UHF Fock matrix expressed in the maximally spin-paired natural bond orbital basis.

Discussion

Spectral Interpretations. The observed spectra leave no doubt about the structure of the radicals that have been generated. To our knowledge, the sizable long-range hyperfine splitting constants observed in the [*n*]staff-3-yl radicals **3** (Table I and Figure 4) exceed any previously known values for such a long-range coupling in saturated hydrocarbon radicals with a formally localized radical center.[18] It is rare to have an opportunity to discuss the coupling of a nominally localized radical center to ζ and ι hydrogens, which involves transmission through six and nine saturated bonds, respectively. Still, the large values are not really surprising, given the huge coupling to the γ hydrogen in the first member of the series. The attenuation factor for the reduction of electron spin density on the terminal proton upon interposition of a bicyclo[1.1.1]pentane cage, going from $n = 1$ to $n = 2$, or from $n = 2$ to $n = 3$, is nearly the same, about 25, and may well represent a good estimate for the attenuation of an electron influence of σ symmetry in [*n*]staffanes in general. This factor is much larger than the factor of 7 for going from a hydrogen atom ($n = 0$) to bicyclo[1.1.1]pent-1-yl ($n = 1$).

The coupling constants to the bridge protons are much smaller than those to the bridgehead proton in the same cage. Interestingly, their magnitude is attenuated by only a factor of about 12 upon going from **3** ($n = 1$) to **3** ($n = 2$). The attenuation factor for going to **3** ($n = 3$) is at least as large, but we were not able to determine its numerical value.

The computed coupling constants are in a surprisingly good agreement with the observations (Table I and Figure 4), considering that neither the UHF method nor a 6-31G* basis set are considered particularly suitable for the calculation of spin density distribution.[28] Given the size of the molecules, and the reasonable agreement with experiment, we propose that the calculations nevertheless represent a reasonable starting point for a qualitative discussion of the observed long-range spin propagation. We note, however, that the attenuation factor for the bridge proton coupling constant is severely overestimated, by a factor of about 5.

It is of interest that ROHF/6-31G* calculation for **3** ($n = 1$) predicts a_H to be only 0.3 and 21.3 G for the β and γ hydrogen, respectively, in very poor agreement with the measured values of 1.3 and 69.4 G.

The optimized geometries are shown in Figure 5. A comparison of the key interatomic distances with those in the parent [*n*]-staffane hydrocarbons, also shown in the figure, is instructive. The only significant differences occur in the radical center carrying cage, which is flattened considerably relative to the parent hydrocarbon, and whose exocyclic bond at the bridgehead is lengthened slightly. In the [1]staff-1-yl radical, the interbridgehead C–C separation is computed to be only 1.814 Å, significantly less than the 1.870 Å calculated for bicyclo[1.1.1]pentane but more than computed previously[21] at the semiempirical level. In the first cage of [2]staff-3-yl, the corresponding numbers are very similar to those in [1]staff-1-yl. In contrast, almost no shortening of the interbridgehead distance is computed for the terminal cage of [2]staff-3-yl, and the structural effects of the radical center clearly die off quite rapidly with distance.

The bridgehead C–H bond length in [1]staffyl is increased slightly over that in the hydrocarbon, as is the bridgehead C–C bond length in [2]staffyl. These, of course, are much stiffer structural parameters, and it is not surprising that the changes are small.

Spin Density Propagation Mechanism—Simple Theory. Taken together, the structural differences support the qualitative rationalization of the propagation of the spin density in terms of σ hyperconjugation, summarized in Figure 6. The importance of the valence-bond structures shown there undoubtedly drops rapidly with the increasing number of missing intercage bonds, and the intervention of the least stable ones can only be detected thanks to the exquisite sensitivity with which EPR detects minute unpaired spin densities.

There is little doubt that it is an oversimplification to attribute all of the spin density appearing on the bridgehead hydrogens in [*n*]staffyl radicals to hyperconjugative transannular interaction, since through-bond coupling surely contributes as well; earlier semiempirical calculations[21] actually suggested that it dominates. For a system in which it proceeds through three sets of two bonds interposed between two bridgehead carbons, it will add constructively[29] three times to the through-space coupling that we

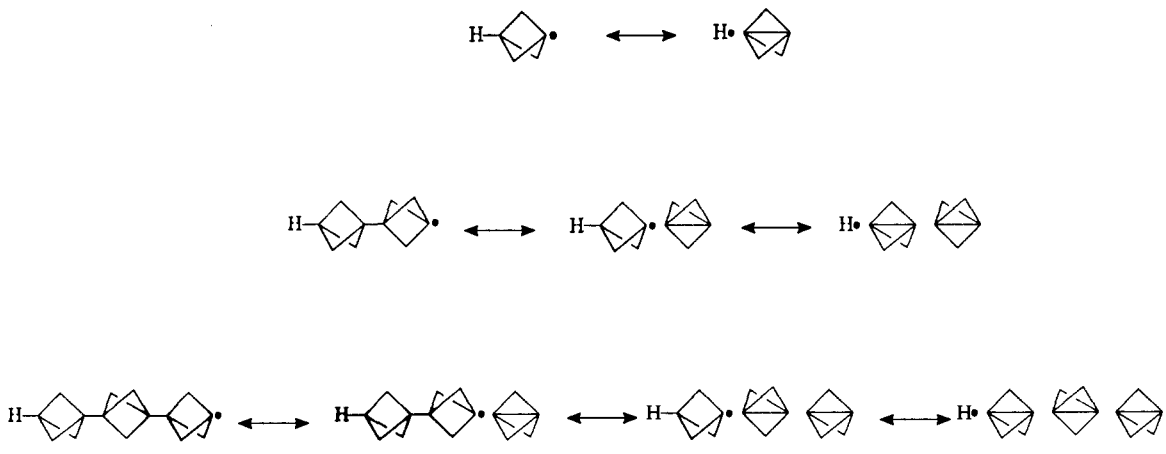

Figure 6. Traditional representation of σ-hyperconjugation in [*n*]staff-3-yl radicals (**3**).

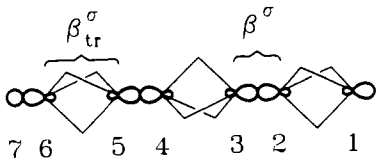

Figure 7. A schematic representation of the atomic orbitals involved in Hückel MO description of spin delocalization. Transannular (β^{σ}_{tr}) and intercage (β^{σ}) resonance integrals are indicated.

have considered so far. It is not simple to unravel the two types of contributions unambiguously, but the fact that the attenuation factor increases from 7 in the first flattened cage to 25 in the more distant cages suggests strongly that the interbridgehead distance is critically important. This argues in favor of the through-space interaction as being quite significant, at least in the first cage, unless the through-bond coupling is extremely sensitive to the CCC valence bond angle. Also the much smaller magnitude of the hyperfine coupling constant of the bridgehead hydrogen in the bridgehead radical with two two-bond and one three-bond through-bond paths, bicyclo[2.1.1]hex-1-yl (**5**), 22.5 G,[30] suggests that the interbridge C–C distance is the critical factor and thus argues for the significance of the through-space σ-hyperconjugative effect. At this level of approximation, we make no attempt to separate the effects of bond delocalization from those of spin-polarization of bonds, but we shall return to this issue below.

In order to provide a qualitative description of the [*n*]staff-1-yl radical at the simple Hückel molecular orbital level (Figure 7), we lump the through-space and through-bond effects together into an effective transannular resonance integral β^{σ}_{tr}, and use β^{σ} for the resonance integral characterizing the intercage C–C bond. The attenuation of the spin density in the hyperconjugated chain of $2n + 1$ σ-symmetry hybrid orbitals located on the molecular axis will be dictated by the ratio $t = \beta^{\sigma}_{tr}/\beta^{\sigma}$. For the sake of simplicity, we assume that the 1*s* orbital on the bridgehead hydrogen has the same properties as the carbon orbitals, although the high 2*s* content of the latter surely makes them quite electronegative.

For $t = 1$, the system would be fully delocalized and equivalent to the π system of allyl, 2,4-pentadiyl, or a longer conjugated polyenyl radical, depending on the number of bicyclo[1.1.1]pentane cages *n* in the [*n*]staff-1-yl. The spin density on each terminal orbital, that located on a bridgehead carbon and that on a bridgehead hydrogen, would be $1/(n + 1)$. σ-Hyperconjugation would be perfectly developed.

For $t = 0$, the system would be fully localized, with a unit spin density on the orbital of a terminal carbon, plus a set of noninteracting C–C single bonds. σ-Hyperconjugation would be absent, and the spin density on the hydrogen orbital would be zero.

For intermediate values of *t*, a Hückel calculation for the singly occupied nonbonding orbital yields a spin density of $(1 - t^2)/(1 - t^{n+2})$ for the terminal carbon orbital and $t^n(1 - t^2)/(1 - t^{n+2})$ for the hydrogen orbital. The attenuation ratio is $t^{-2}(1 - t^{n+4})/(1 - t^{n+2})$ per cage. For the present purposes, this can be approximated by t^{-2}. For cages distant from the radical center, the experimentally determined attenuation ratio is about 25, and we conclude that $t = 1/5$. In this simple model, the transannular resonance integral β^{σ}_{tr} in an undistorted bicyclo[1.1.1]pentane cage is thus equal to about one-fifth of the resonance integral β^{σ} of the intercage C–C bond. For the radical center carrying first cage, the attenuation ratio is only about 7, so that in such a flattened cage the transannular resonance integral β^{σ}_{tr} equals $0.4\beta^{\sigma}$. However, this value is almost certainly overestimated by the neglect of the lower electronegativity of the hydrogen orbital relative to the carbon orbitals. For the more distant cages the error introduced by this neglect will be much smaller, since the nonbonding orbital then has only a small coefficient on the hydrogen atom.

Spin Density Propagation Mechanism—Natural Bond Orbital Analysis. In order to separate the through-space and through-bond effects, we take recourse to the approximate ab initio UHF wave function and natural bond orbital (NBO) analysis.[31] Although NBO analysis has been used previously to separate through-space and through-bond effects in orbital interactions,[32] to our knowledge, this procedure has not been used so far for the analysis of the mechanism of spin density propagation through a molecule. The required generalization of the standard procedure appears fairly straightforward.[33] Other methods such as the one based on corresponding orbitals have been used in previous spin density propagation studies[34] to separate the spin polarization and spin delocalization mechanisms but cannot be easily applied to our primary goal, the separation of the through-space and through-bond effects. The algorithm that we have chosen to use is based on the notion that a maximally spin-paired fully localized natural bond orbital (MSP-NBO) wave function can be written by using a basis set consisting of an occupied (Rα) and a vacant (R*β) spin orbital fully localized at the radical center and of two pairs of fully localized spatially identical spin orbitals located on each bond, one for the spin α and one for the spin β. One pair ($\sigma_{ij}\alpha$, $\sigma_{ij}\beta$) describes the bonding bond orbital σ_{ij}, the other ($\sigma^*_{ij}\alpha$, $\sigma^*_{ij}\beta$) the antibonding bond orbital σ^*_{ij}. If all the bonding bond orbitals σ_{ij} are doubly occupied, and only the spin orbital Rα on the radical center is occupied, but not R*β, spin density originates exclusively from the contributions due to the one electron in Rα. On distant atoms, such as the bridgehead hydrogen in **3** ($n = 1$), these contributions are negligibly small. Such a maximally spin-paired localized wave function corresponds to the fully classical interpretation of the structural formula **3** ($n = 1$). This MSP-NBO wave function will represent our reference point for the description of the real spin density distribution in the radical. We shall be able to examine how the introduction of various mechanisms of interaction between the bond spin orbitals, $\sigma_{ij}\alpha$ and $\sigma_{ij}\beta$, the antibonding spin orbitals, $\sigma^*_{ij}\alpha$ and $\sigma^*_{ij}\beta$, and the localized orbitals at the radical center, Rα and R*β, produce the actual UHF wave function with a delocalized spin density.

The MSP-NBOs could be chosen in several ways. Perhaps the most appropriate theoretically would be the localization of the spin-unpolarized orbitals obtained by an SCF calculation on a radical that places a "half-electron" of spin and a "half-electron" of spin β into the singly occupied orbital.[35] Given programs already available, a more expedient procedure is the usual NBO calculation starting from a UHF or ROHF wave function, followed by the averaging of the α and β spin electron densities. We suspect that all three procedures will yield very similar results in practice and have verified that the latter two indeed do. In the following, we describe the results obtained with MSP-NBOs generated by the averaging of ROHF electron density matrices for α and β spin.

When the UHF Fock matrix is written in the MSP-NBO basis, it contains nonzero off-diagonal elements. After diagonalization, the UHF spin-orbitals are recovered, and when occupied appropriately, they produce the normal UHF spin density distribution. For **3** ($n = 1$), this yields a hyperfine coupling constant $a_H = 56.5$ G for the bridgehead hydrogen, while the MSP-NBO wave

(28) For a recent discussion, see: Chipman, D. M. *Theor. Chim. Acta* **1992**, *82*, 93.

(29) Paddon-Row, M. N. *Acc. Chem. Res.* **1982**, *15*, 245. Verhoeven, J. W. *Recl. Trav. Chim. Pays-Bas* **1980**, *99*, 369.

(30) Kawamura, T.; Yonezawa, T. *J. Chem. Soc., Chem. Commun.* **1976**, 948.

(31) Reed, A. E.; Curtiss, L. A.; Weinhold, F. *Chem. Rev.* **1988**, *88*, 899.

(32) Jordan, K. D.; Paddon-Row, M. N. *Chem. Rev.* **1992**, *92*, 395. Liang, C.; Newton, M. D. *J. Phys. Chem.* **1992**, *96*, 2855.

(33) A more explicit mathematical description of the procedure will be published elsewhere: Balaji, V.; Michl, J., manuscript in preparation. The usual NBO wave function[31] is not suitable for our purposes, particularly for distinguishing between through-space and through-bond spin density propagation. Since it represents merely another form of writing the ordinary UHF or ROHF wave function, it contains delocalized spin density and its NBOs are spin-polarized. Even if all off-diagonal elements of the UHF Fock matrix written in the basis of these NBOs are deleted, the spin density on the bridgehead hydrogen in **3** ($n = 1$) remains huge. Clearly, the deletion of the off-diagonal elements in the usual NBO procedure inhibits spin density propagation by bond delocalization but not by bond spin polarization.

(34) Marcellus, D. H.; Davidson, E. R.; Kwiram, A. L. *Chem. Phys. Lett.* **1975**, *33*, 522.

(35) Jørgensen, P.; Bellum, J. *Mol. Phys.* **1973**, *26*, 725.

function, which corresponds to the deletion of all off-diagonal elements, yields a_H = 0.02 G (Table II).

There are four classes of off-diagonal elements in the Fock matrix, corresponding to four mechanisms of spin density delocalization: through-space spin polarization (TSP), through-bond spin polarization (TBP), through-space delocalization (TSD), and through-bond delocalization (TBD). The distinction between spin polarization and spin delocalization defined in this fashion is similar to but not identical with the usual way[34] of defining these two unobservable and therefore somewhat arbitrarily definable contributions to spin density propagation in a molecule.

The first two types of matrix elements permit no delocalization of the individual bond orbitals, only their spin polarization. These are the matrix elements between a bonding and an antibonding spin orbital of the same spin localized on the same bond, $\sigma_{ij}\alpha-\sigma^*_{ij}\alpha$ and $\sigma_{ij}\beta-\sigma^*_{ij}\beta$. In the general case, the diagonal elements (energies) of $\sigma_{ij}\alpha$ and $\sigma_{ij}\beta$ are different, since an electron in the bond spin orbital $\sigma_{ij}\beta$ has a repulsion of $J(\sigma_{ij},R)$ with an electron in the radical center orbital Rα, while an electron in spin orbital $\sigma_{ij}\alpha$ of the same bond has a repulsion of only $J(\sigma_{ij},R) - K(\sigma_{ij},R)$ with the electron in Rα, where J and K are the usual Coulomb and exchange integrals. Thus, even if the off-diagonal elements were the same in the α and the β spin space, they will cause a different degree of mixing of the bond and antibond spin orbitals in the α and the β spin space, and thus a spin polarization of the bond even in the absence of any bond delocalization.

Through-space spin polarization (TSP) of a bond results from asymmetry of its location relative to the radical center orbital Rα, with excess α spin accumulating at that end of the bond that overlaps more with Rα. Since the exchange integral $K(\sigma_{ij},R)$ falls off rapidly with increasing distance between the bond ij and the orbital Rα, the TSP mechanism is normally important only for bonds adjacent to the radical center. In **3** (n = 1), due to the abnormally short separation of the carbon of the bridgehead CH bond from the radical center, the through-space spin polarization of this bond is large as well. The introduction of the matrix elements $\sigma_{CH}-\sigma^*_{CH}$ in the α and β space alone produces a_H = 32.6 G on the bridgehead hydrogen, between half and two-thirds of the UHF total.

In a chain of bonds, spin polarization without delocalization can occur successively through a series of bonds (through-bond spin polarization, TBP): the bond adjacent to the radical center containing an α electron will be polarized with excess β spin on its other end; this will induce excess β spin at the nearby end of the next adjacent bond, etc. This effect falls off rapidly with the number of bonds in the chain, and adding the three through-bond spin polarization paths to the through-space bond spin polarization path in **3** (n = 1) increases a_H merely from 32.6 to 32.7 G. The TBP contribution is clearly negligible.

The other two types of matrix elements correspond to the two mechanisms of spin density delocalization that depend on bond delocalization; by themselves these do not produce bond spin polarization. In **3** (n = 1), they are responsible for less than half of the UHF total.

The through-space bond delocalization (TSD) mechanism of spin transfer to bond σ_{ij} is due to the matrix elements Rα-$\sigma_{ij}\alpha$, Rα-$\sigma^*_{ij}\alpha$, R*β-$\sigma_{ij}\beta$, and R*β-$\sigma^*_{ij}\beta$, i.e., to the direct hyperconjugation of the CH bond with R. In **3** (n = 1), this mechanism alone, not permitting the CH bond to spin-polarize, only produces a_H = 6.88 G. It produces a_H = 39.5 G when the CH bond is allowed to spin-polarize, i.e., when the $\sigma_{CH}-\sigma^*_{CH}$ elements are kept. This is to be compared with a_H = 32.6 obtained if the spin-polarization of the CH bond is induced only by through-space interaction with the radical center R. Thus, the two types of through-space interaction (TSP + TSD) together account for between two-thirds and three-quarters of the total UHF value of a_H.

The through-bond delocalization (TBD) mechanism corresponds to the presence of a chain of matrix elements between the radical center orbitals Rα and R*β and the σ_{ij}, σ^*_{ij} bond orbitals: $\sigma_{ij}-\sigma_{kl}$, $\sigma_{ij}-\sigma^*_{kl}$, $\sigma^*_{ij}-\sigma_{kl}$, $\sigma^*_{ij}-\sigma^*_{kl}$, R$-\sigma_{kl}$, R$-\sigma^*_{kl}$, R*$-\sigma_{kl}$, R*$-\sigma^*_{kl}$, etc. In **3** ($n$ = 1), the three paths available for the through-bond delocalization mechanism of spin density transfer to the bridgehead hydrogen, not allowing the CH bond to spin-polarize, only yield a_H = 6.45 G. If the CH bond is allowed to spin-polarize, the introduction of the through-bond delocalization mechanism brings a_H from the value of 32.6 G, due to through-space spin-polarization alone, to 39.0 G.

It is possible to subdivide the through-bond delocalization mechanism further into paths due purely to geminal interactions (those between adjacent bonds), those due to "perivalent" interactions (those between bonds or radical centers attached to the two opposite termini of a single bond, as in an anti-periplanar or syn-periplanar arrangement) and, in molecules of arbitrarily large size, also longer range interactions. In **3** (n = 1), such longer range interaction of the bridgehead CH bond and the radical center is identical to the through-space bond delocalization interaction. In this molecule, the three chains of geminal interactions yield a_H = 2.36 G if the CH bond is not allowed to spin-polarize, and a_H = 35.4 G when it is. The perivalent interactions yield a_H = 1.95 G if the CH bond is not allowed to spin-polarize, and a_H = 34.2 G when it is. It will be recalled that the through-space spin polarization of the CH bond yields a_H = 32.6 G all by itself. It is seen that geminal and perivalent interactions contribute comparably to the through-bond delocalization mechanism and together provide about one-eighth of the total UHF result.

The fact that the contributions of the four individual mechanisms do not add up to the UHF value is not surprising; the mechanisms interfere in a coherent manner and exact additivity can be expected only in the zeroth approximation.

The identification of the through-space TSP and TSD interactions as primarily responsible for the large a_H value is obvious upon inspection of Table II. It is in accord with the qualitative arguments given above and with calculations in which the transannular separation of the two bridgehead carbon atoms in **3** (n = 1) was varied by 0.1 Å in either direction. For a 1.714-Å separation, the UHF value increased to a_H = 69.2 G. For a 1.914-Å separation, it decreased to a_H = 47.0 G, demonstrating the expected large sensitivity.

Conclusions

The [n]staffane skeleton has an impressive ability to propagate spin density of σ symmetry over a long distance. The attenuation factor is about 25 per undistorted bicyclo[1.1.1]pentane cage. In a simple Hückel model of σ hyperconjugation, this corresponds to a ratio t = 1/5 of the effective transannular (β^σ_{tr}) to the intercage (β^σ) resonance integrals. This value can now be used in applications of the simple model to the interpretation of other electronic structure properties of the [n]staffane spacers.

At a more sophisticated level of MSP-NBO analysis of an ab initio UHF wave function for the first member of the series, **3** (n = 1), close to three-quarters of the electron spin density on the bridgehead hydrogen atom are seen to originate from through-space effects, mostly bond spin-polarization, about one-eighth from through-bond effects, almost exclusively bond delocalization, and the remainder is due to interference between the artificially separated mechanisms.

Acknowledgment. This work was supported by a grant from the National Science Foundation (DMR 8807701). The purchase of a computer was supported by National Science Foundation (CHE 9022151). We thank Prof. Frank Weinhold for the NBO program and valuable comments on the NBO analysis. We are grateful to Dr. Piotr Kaszynski for preparing samples of 1-bromobicyclo[1.1.1]pentane and *tert*-butyl 3-(methoxycarbonyl)bicyclo[1.1.1]pentane-1-peroxycarboxylate.